A Phase I Trial Combining High-Dose ^{90}Y-Labeled Humanized Anti-CEA Monoclonal Antibody with Doxorubicin and Peripheral Blood Stem Cell Rescue in Advanced Medullary Thyroid Cancer

Robert M. Sharkey, PhD[1]; George Hajjar, MD[1]; Dion Yeldell, BS[1]; Arnold Brenner, DO[1]; Jack Burton, MD[1]; Arnold Rubin, MD[2]; and David M. Goldenberg, ScD, MD[1]

[1]*Center for Molecular Medicine and Immunology, Garden State Cancer Center, Belleville, New Jersey; and* [2]*St. Joseph's Hospital and Medical Center, Paterson, New Jersey*

This trial determined the pharmacokinetics, dosimetry, and dose-limiting toxicity of ^{90}Y-hMN-14 IgG (humanized anticarcinoembryonic antigen [CEA, or CEACAM5] monoclonal antibody; labetuzumab), combined with doxorubicin and peripheral blood stem cell (PBSC) support in advanced medullary thyroid cancer (MTC) patients. **Methods:** Fifteen patients received an infusion of ^{111}In-hMN-14 IgG. One to 2 wk later, 14 patients received ^{90}Y-hMN-14 IgG, starting at 740 MBq/m^2, followed 24 h later with a fixed intravenous bolus dose of doxorubicin (60 mg/m^2). Preharvested PBSCs were reinfused when the ^{90}Y activity in the body was ≤111 MBq/m^2. **Results:** The mean red marrow dose estimated for the ^{90}Y-hMN-14 IgG was 1.65 ± 0.59 mGy/MBq (n = 11), with normal organs ranging from ~2.3 to 4.4 mGy/MBq. Eighty percent of all known lesions (125/156), including 78 of 79 bone and 16 putatively occult lesions, were targeted. The average radiation dose to the tumor was 15.1 ± 10.8 mGy/MBq (55.8 ± 39.8 cGy/mCi) ^{90}Y-hMN-4 IgG (n = 29 tumors in 8 patients), with a majority of the lesions receiving >2,000 cGy at an administered dose of ≤1,480 MBq/m^2. The average tumor-to-red marrow, tumor-to-liver, tumor-to-lungs, and tumor-to-kidneys ratios were 15.0 ± 11.0, 5.1 ± 3.6, 6.9 ± 6.1, and 9.0 ± 8.7, respectively. Cardiopulmonary toxicity was dose limiting at 1,850 MBq/m^2. Minor responses were noted in 2 patients and 1 patient had a partial response (68% reduction in local and hepatic metastatic disease). **Conclusion:** This treatment combination was well tolerated with complete recovery of blood counts and reversible nonhematologic toxicities at the maximum tolerated dose of 1,480 MBq/m^2. Evidence of antitumor response in these patients with advanced cancer was modest, but encouraging; this type of treatment may be more successful if applied to more limited, earlier-stage disease.

Key Words: carcinoembryonic antigen; medullary thyroid cancer; radioimmunotherapy; chemotherapy; dosimetry; monoclonal antibody

J Nucl Med 2005; 46:620–633

Medullary thyroid cancer (MTC) accounts for approximately 5%–10% of all thyroid cancers and arises from the parafollicular cells (C cells) of the thyroid gland (*1*). C cells produce calcitonin, a peptide with a role in calcium metabolism and bone physiology that is also a useful tumor marker indicating the presence of functional C cells. This disease can occur as a sporadic tumor or as part of a multiple endocrine neoplasm syndrome, which has a familial distribution (*2*). Surgery is the only curative therapeutic approach. However, once there is metastatic spread, this disease is essentially incurable. External-beam radiation therapy has been used as a palliative modality to control symptomatic disease, albeit with limited success (*3*). Different chemotherapeutic agents also have been studied, with doxorubicin (Dox) being the most widely used agent, alone or in chemotherapy combinations (*4–9*). Dox also has the property of being a radiosensitizer when used in combination with radiotherapy (*10*).

In addition to calcitonin, 70%–90% of MTC tumors express carcinoembryonic antigen (CEA) on their surface (*11*), making the use of anti-CEA monoclonal antibodies attractive for imaging and therapy of MTC. Excellent targeting was reported by our group and others using directly radiolabeled anti-CEA monoclonal antibodies in patients with metastatic MTC (*12–14*) and by others using a bispecific anti-CEA x anti-DTPA (diethylenetriaminepentaacetic acid) antibody pretargeting procedure (*15*). Therapeutic responses were found using both nonmyeloablative doses (*16*) as well as myeloablative doses with peripheral blood stem

Received Sep. 15, 2004; revision accepted Nov. 17, 2004.
For correspondence or reprints contact: David M. Goldenberg, ScD, MD, Garden State Cancer Center, 520 Belleville Ave., Belleville, NJ 07109.
E-mail: dmg.gscancer@att.net.

cell (PBSC) rescue (*17*) of a murine, ^{131}I-labeled anti-CEA $F(ab)_2$ in patients with metastatic MTC. This murine monoclonal antibody was subsequently humanized (hMN-14) and shown to have similar targeting properties and reduced immunogenicity compared with the murine MN-14 IgG (*18*). The hMN-14 IgG was selected for use in this trial in combination with ^{90}Y because of ^{90}Y's longer path length compared with ^{131}I (which is expected to deliver a more homogeneous radiation dose to the tumors) and its ability to be infused on an outpatient basis (because of being a pure β-emitter). ^{90}Y was stably linked to the anti-CEA IgG using a DOTA (1,4,7,10-tetraazacyclododecane-*N,N′,N″,N‴*-tetraacetic acid) chelate (*19*). Because preclinical studies in mice bearing a human MTC xenograft indicated that a combination of Dox with radiolabeled anti-CEA antibodies could improve therapeutic responses (*20–22*), Dox was added to the treatment regimen. In addition, all patients were required to have PBSCs harvested before treatment, in an attempt to circumvent dose-limiting hematologic toxicity associated with radiolabeled antibody therapy and to deliver a higher radiation-absorbed dose to targeted tumors. The primary aim of this trial was to examine the pharmacokinetic properties, organ and tumor dosimetry, and dose-limiting toxicity (DLT) of this combined treatment regimen, and to assess any antitumor responses in these patients.

MATERIALS AND METHODS

Antibody Preparation and Radiolabeling

Humanized MN-14 (Immu-14 or labetuzumab) IgG and DOTA-conjugated hMN-14 IgG were provided by Immunomedics, Inc. A minimum of 10 mg of the DOTA-hMN-14 was used in the preparation of the radiolabeled products with the initial ratio not exceeding 222 MBq/mg. For radiolabeling, the chelate-conjugate (in 0.25 mol/L sodium acetate buffer, pH 5.5) was added to the isotope vial supplied by radionuclide manufacturer. $^{111}InCl_3$ and $^{90}YCl_3$ were purchased from either Perkin-Elmer or IsoTex. Radiolabeling was performed at 43°C for 5–10 min followed by a brief incubation with an excess of DTPA at room temperature, to scavenge nonantibody-bound radiometal. The final product was sterilely filtered in a vial containing saline to meet the prescribed radioactivity dose for each patient (±10%). Quality-assurance testing included instant thin-layer chromatography (ITLC) for nonantibody-bound radionuclide (i.e., DTPA bound) and size-exclusion high-performance liquid chromatography (HPLC) (300 × 7.8 mm Bio-Sil SEC250 column with guard; Bio-Rad Laboratories) of the radiolabeled product alone and after addition of a 10-fold molar excess of CEA (Scripps Laboratories, Inc.) to assess the immunoreactive fraction. These studies showed that the final radiolabeled products had 2.6% ± 0.5% and 5.7% ± 3.1% unbound ^{111}In or ^{90}Y, respectively, by ITLC and 2.8% ± 2.7% and 2.8% ± 3.1% aggregates for the ^{111}In- and ^{90}Y-radiolabeled IgG, respectively, by size-exclusion HPLC. Other studies have shown that ^{111}In and ^{90}Y are both very stable when bound by DOTA-conjugated antibodies (*19*). The immunoreactive fraction was ≥90%.

Antibody Administration

Before injection of the ^{111}In- and ^{90}Y-labeled antibody, the patients first received a predose of unconjugated, unlabeled hMN-14 IgG with the intent to reduce the potential for complexation of the radiolabeled antibody with circulating CEA. The amount of unlabeled antibody administered equaled the total antibody protein (0.75 mg/kg) minus the amount of DOTA-hMN-14 IgG used to provide the radiolabeled antibody dose. The amount of unlabeled antibody given ranged from 21.6 to 72.5 mg, which represented 42.5%–93.8% of the total antibody administered dose. The amount of unlabeled antibody preinfused for the second injection was within 10% of the first injection for patients through patient 1799. Thereafter, the amount of unlabeled antibody preinfused for the second injection was 25%–65% less than that in the first injection because of the need to use additional DOTA-hMN-14 to provide the higher ^{90}Y-doses as well as the inclusion of patients who were coinfused with ^{111}In-DOTA-hMN-14. The unconjugated antibody was added to a buretrol containing 20–30 mL of saline and infused over approximately 30–50 min. The radiolabeled antibody was infused immediately at the conclusion of the unlabeled antibody infusion over another 15–30 min, except in 5 patients for whom there was a brief interval of 5–23 min between the 2 infusions. All antibody infusions were initiated without premedication, starting slowly with about 10% of the total dose infused over the first 5–10 min and then, as long as vital signs remained stable, the remaining dose was infused. Vital signs were then measured at 1, 2, and 24 h after the end of the radiolabeled antibody infusion.

Patient Selection and Registration

This clinical trial was conducted with Institutional Review Board approval and an investigator-initiated Investigational New Drug application from the Food and Drug Administration. Patients with histologic or cytologic diagnosis of MTC (sporadic or familial) were studied. Eligibility criteria included (a) unresectable locoregional MTC or distant metastases; (b) presence of measurable or evaluable disease by CT, with targeting of at least one cancer lesion seen on the CT scan in the diagnostic imaging study; (c) adequate PBSC or bone marrow harvest before receiving treatment; (d) white blood cells > 3,000/mm^3, granulocytes > 1,500/mm^3, and platelets > 100,000/mm^3; (e) bilirubin ≤ 2 mg/dL and creatinine < 1.5 × the institutional upper limit of normal; (f) a cardiac ejection fraction of at least 50% and pulmonary function parameters (forced vital capacity [FVC] and diffusing capacity of lung for carbon monoxide [DLCO]) of at least 60% of predicted for their age; (g) age ≥16 y; and (h) Karnofsky performance status of ≥70 (Eastern Cooperative Group [ECOG] score 0–2). Patients who had known brain metastases or prior radiation therapy to >35% of their bone marrow, or who had received prior therapy with >240 mg/m^2 of Dox or who showed progression after prior Dox treatment, were excluded. All patients were mentally responsible and provided a written informed consent.

Table 1 lists some of the demographics of the patients enrolled in this trial, including their age, sex, sites of disease at enrollment, and baseline blood CEA and calcitonin levels. A total of 15 patients (11 men, 4 women; age range, 16–75 y) were enrolled and received a diagnostic imaging study, but only 14 received treatment, because the liver enzymes of 1 patient increased in the week before receiving the therapy dose, making him ineligible for the ^{90}Y-hMN-14 treatment.

Trial Design

The scheme in Figure 1 shows the treatment plan. All patients had PBSCs harvested after mobilization with granulocyte colony-stimulating factor (G-CSF). At least 2 × 10^6 CD34$^+$ cells/kg were

TABLE 1
Patient Demographics

Patient no.	Age (y)	Sex	Sites of disease at study entry	Prior treatment (time from RAIT)	Baseline tumor markers		MBq/m^2 ^{90}Y-hMN-14 (MBq)
					CEA (ng/mL)	Calcitonin (pg/mL)	
1779	41	M	Neck, lungs	S (11 mo)	200	ND	740 (1,654)
1782	59	M	Neck, lungs, bone	S (8 mo) XRT (3 sites) (2–5 mo)	6,400	56,170	740 (1,610)
1785	51	M	Neck, Med	S (5 mo)	380	5,224	740 (1,606)
1789	70	M	Neck, Med, lungs	S (5 mo)	12	891	1,110 (2,642)
1790	32	M	Med, liver	S (32 mo) Neck XRT (16 mo)	1,800	<14	NT
1791	41	F	Parotid gland	Multiple S (2–15 y)	280	2,173	1,110 (2,253)
1796	70	F	Thyroid, Med, liver	S (7 mo) Taxol/carboplatin (2 mo)	1,180	49,411	1,110 (1,887)
1799	42	M	Neck, Med	S (3 y) ^{131}I ablation + XRT (3 y)	5.7	15,541	1,480 (3,034)
1812	16	M	Neck, lungs	S (2 mo)	240	51,194	1,480 (1,672)
1818	75	M	Neck, bone	S (4 mo)	3,650	69,780	1,480 (2,967)
1827	63	F	Neck, Med	S (6 mo)	4.6	4,784	1,850 (3,700)
1831	19	F	Lungs, liver, bone	XRT (2 mo)	156	5,114	1,850 (2,997)
1853	41	M	Neck, lungs, abdomen, liver	None	260	13,118	1,850 (3,193)
1887	71	M	Neck, Med	S (1–12 y)	33	1,572	1,850 (3,574)
1889	60	M	Lungs, Med, liver	S (10 y) XRT (9 y)	320	15,071	1,850 (3,563)

RAIT = radioimmunotherapy; S = surgery; ND = not done; XRT = external-beam therapy; Med = mediastinum; NT = not treated.

required. Patients then received ~222 MBq of ^{111}In-hMN-14 IgG. Scintigraphy and blood pharmacokinetics were obtained after the ^{111}In-hMN-14 infusion to predict the pharmacokinetics and radiation-absorbed doses for the subsequent ^{90}Y-hMN-14 infusion. These data also were used to predict when the total-body ^{90}Y radioactivity level would be <111 MBq/m^2 and, at this time, the PBSCs were reinfused. Treatment was given only when targeting of a confirmed tumor was established after the ^{111}In-hMN-14 injection and the predicted time for reinfusion of the PBSCs was ≤2 wk after receiving the ^{90}Y-hMN-14. In addition, dosimetry estimates had to show that the predicted absorbed dose to the liver would not exceed 3,000 cGy, or 2,000 cGy to the lungs and kidney at the prescribed ^{90}Y-hMN-14 dose level. Treatment with ^{90}Y-hMN-14 was given 6–8 d after ^{111}In-hMN-14 in most patients (12–13 d in 4 patients), and at least 14 d after the final G-CSF injection was given during the harvesting of the PBSCs. One day after the ^{90}Y-hMN-14 therapy infusion, a fixed dose of Dox (60 mg/m^2) was given as an intravenous bolus. Dose escalation was based on body surface area (MBq/m^2), with Table 1 listing the administered ^{90}Y-hMN-14 radioactivity in the 14 patients who received treatment. DLT was defined as grade 3 nonhematologic toxicity (except for alopecia, for which any grade was acceptable, or nausea and vomiting, for which grade 4 toxicity of 7 d was acceptable), grade 4 neutropenia or thrombocytopenia of >21-d duration, or anemia requiring transfusion support for >42 d. Toxicities were graded according to the National Cancer Institute Common Toxicity Criteria, version 2.0. Three patients were treated at each dose level, and only after all patients had completed 8 wk of follow-up with no DLT was the dose escalated to the next level. If any one of the 3 patients treated at a dose level developed DLT, up to 3 additional patients were to be studied at that dose level. However, if ≥2 patients at any dose level developed DLT, no further escalation was permitted. Patients were to be monitored for hematologic and nonhematologic toxicity for a minimum of 3 mo and, whenever possible, up to 5 y. Two patients had 2–3 mo of follow-up, whereas 4 patients had 3–6 mo, 5 had 6–9 mo, and 3 had >1-y follow-up.

Pharmacokinetics, Imaging, and Dosimetry

Whole-body (WB) clearance was determined after the ^{111}In-hMN-14 IgG infusion by serial WB γ-camera imaging, typically starting from within 1 h of the end of the infusion, but before voiding, until the ^{90}Y-hMN-14 therapy infusion 6–8 d later. The ^{111}In-IgG WB effective half-life ($t_{1/2}$) and residence times were computed from monoexponentially curve-fit data (6–8 time intervals). WB clearance was also estimated for ^{90}Y-hMN-14 using this same dataset by assuming the biologic clearance of the ^{111}In- and ^{90}Y-products was identical and then deriving the predicted effective data for ^{90}Y-hMN-14. Three patients received a second ^{111}In-hMN-14 dose (~370 MBq) with the ^{90}Y-hMN-14 therapy infusion. This second ^{111}In-hMN-14 infusion was performed to compare the pharmacokinetics and biodistribution of the sequential injections and to obtain a preliminary assessment of how well the first ^{111}In-hMN-14 could be used to extrapolate the pharmacokinetics and dosimetry for a second injection given approximately 1 wk later (the therapy dose was administered 7–8 d after the first ^{111}In-hMN-14 injection in these 3 patients). In these 3 patients, serial WB imaging was performed at time points similar to those used after the first ^{111}In-hMN-14 infusion. These data were again fit with a monoexponential curve to describe WB clearance. In addition, urine was collected over 7 d in 2 patients and 3 d in 1 patient after the therapy injection, and the ^{111}In and ^{90}Y activities

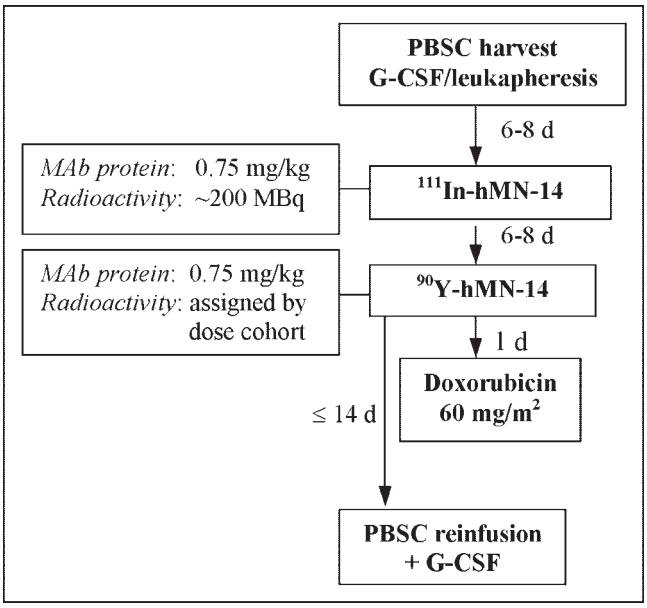

FIGURE 1. Treatment plan. Each patient received a pretherapy imaging study with ^{111}In-hMN-14 IgG. This study was used to (a) confirm targeting of at least 1 index lesion, (b) estimate radiation-absorbed doses for ^{90}Y-hMN-14 to ensure that the dose to liver would not exceed 3,000 cGy and the lung and kidney dose would not exceed 2,000 cGy at prescribed ^{90}Y-hMN-14 administered dose, and (c) to verify that amount of ^{90}Y radioactivity remaining in the whole body would be ≤3 mCi/m^2 no later than 14 d in order to reinfuse PBSCs within this time. PBSCs were reinfused between 7 and 12 d, depending on dose level. G-CSF = granulocyte colony-stimulating factor; Mab = monoclonal antibody

were determined. Comparisons were then made to WB clearance data derived from the pretherapy ^{111}In-hMN-14 injection by external scintigraphy, from external scintigraphy of the ^{111}In-hMN-14 given together with the ^{90}Y-hMN-14 dose, and from the urinary clearance of ^{111}In and ^{90}Y radioactivity measured after the second infusion.

Blood clearance was determined by counting the radioactivity in serial serum samples. Typically, 5–9 samples were collected over a 7-d period (a minimum of 5 samples was required). ^{111}In activity was determined by γ-scintillation counting, whereas ^{90}Y activity was determined using Cerenkov counting in a β-scintillation counter. In the case in which ^{111}In and ^{90}Y activities were coinfused, the ^{111}In activity was corrected for ^{90}Y scatter in the ^{111}In window. The volume of the serum sample was corrected to that of the whole blood using the baseline hematocrit of the patient, and then these data were processed using CONSAM (conversational SAAM version 3.0; Resource Facility of Kinetic Analysis) software examining both a monoexponential and a biexponential fit. Serum obtained within 1 and 24 h after each infusion was also examined in most patients by size-exclusion HPLC equipped with an in-line radiation detector or through the quantitation of radioactivity by a fraction collector in 0.2-mL fractions.

After each ^{111}In-hMN-14 infusion, anterior and posterior planar images of 3 or 4 regions (e.g., head/neck, chest, abdomen, and pelvis) were also obtained using a dual-head Solus camera (ADAC Laboratories) fitted with a medium-energy collimator. Planar images (5–10 min per view) were obtained starting 2–4 h after injection, with serial images done on at least 3 separate days between 1 and 5–7 d after the injection. One or 2 SPECT images were obtained typically between 48 and 72 h. SPECT was performed using a 64 × 64 matrix with 64 or 128 projections over 360° (average counts per projection = 60,000). Targeting sensitivity was assessed by side-by-side comparison of radioantibody scans and anatomic scans (usually CT).

Planar views were used for drawing regions of interest (ROIs) for the major organs, from which time–activity curves and radiation-absorbed doses were derived. ROIs were drawn for the kidneys, liver, lungs, and spleen. Dosimetry is reported only for those organs that were not involved with or masked by overlying or underlying tumor. ROIs for red marrow were based primarily on the lumbar spine, but the sacrum was used in the event of tumor involvement in the lumbar region. There were 2 patients in whom overlying tumor masked both the sacral and the lumbar regions. In this instance, the red marrow dose was calculated only from the serum clearance data, using the hematocrit to approximate the radioactivity in the whole-blood volume, and then applying a factor of 0.36, which represents an average red marrow-to-blood ratio (*23*). Activity quantitation from the images was determined by 2 methods—the buildup factor method (BFM) used in 10 patients (*24*) and the modified geometric mean method (MGMM) used in 5 patients (*25*). Because we had reported previously that radiation dose estimates derived from these 2 methods were similar for all normal tissues except the lungs (*26*), the radiation-absorbed dose for all organs, except the lungs, was averaged. Each set of organ time–activity data was fit to a mono-, bi-, or triexponential function using CONSAM, but most often a triexponential function was selected. For each method, dividing the area under the curve by the injected activity derived a residence time that was used in MIRDOSE3 (*27*) to calculate the radiation-absorbed dose. Absorbed doses were calculated for ^{90}Y from the ^{111}In-hMN-14 imaging study by using the biologic clearance curves for ^{111}In-hMN-14 and substituting the physical half-life of ^{90}Y to derive an effective clearance curve for ^{90}Y. Organ volumes were taken from MIRD (*28*). For tumor dosimetry, volumes were derived from bidimensional CT measurements, using the average of the 2 diameters to derive a radius, and, from this, a spheric volume was calculated. Time–activity curves for the tumors were fit by a trapezoidal model. The integral for the tumor time–activity curves was multiplied by the tumor S factor that was interpolated from S values of the nodule module in CONSAM software (*27*).

Toxicity and Tumor Response

Hematologic toxicity was monitored by complete blood counts performed approximately 3 times per week after reinfusion of PBSCs or bone marrow, until counts had recovered to ≤grade 2, at which time sampling was performed twice weekly until counts stabilized for at least 2 consecutive weeks. Nonhematologic toxicities were monitored, whenever possible, as follows: renal and hepatic toxicities were monitored by serum biochemistry profiles; cardiac and pulmonary toxicities were monitored by multiple gated acquisition (MUGA) scans and pulmonary function tests were performed at 8, 24, and 36 wk after treatment, and every 6–12 mo after that if the patient developed toxicity until recovery; neurologic and gastrointestinal (GI) toxicities were monitored by history and physical examination. Since all patients were referred to us from outside the local region, follow-up monitoring was performed primarily by the referring physician, and we maintained regular contact with the patients and their physicians and obtained copies

of their medical records on a regular basis. Antitumor responses were assessed by serial CT at 1 and 3 mo after therapy and thereafter at 6-mo intervals or until progression occurred. Responses were judged according to ECOG criteria, using baseline studies obtained within 4 wk of the ^{111}In-hMN-14 study. Blood CEA and calcitonin levels were determined at 1 mo after treatment and at monthly intervals for 1 y whenever possible, or until progression.

Human Anti-Humanized Antibody (HAHA) Determination

A blood HAHA titer was determined for all patients at baseline. Follow-up testing was performed at 2, 4, 8, and 12 wk after treatment, whenever possible. The titer was determined by using 1 of 2 assays: the HPLC assay ($n = 10$), and later the enzyme-linked immunosorbent assay (ELISA) ($n = 5$). These methods were described in detail previously by Hajjar et al. (*29*)

TABLE 2
Effective WB Clearance (Hours)*

Patient no.	Injection 1 (^{111}In-hMN-14 alone): ^{111}In-hMN-14 external scintigraphy	Injection 2 (^{111}In- and ^{90}Y-hMN-14 coinjected)		
		^{111}In-hMN-14		
		Urine	External scintigraphy	^{90}Y-hMN-14, urine
1827	61.5	62.3	59.3	57.2
1831	56.9	61.8	62.4	58.3
1889	61.9	61.5	61.9	58.4

*Determined by external scintigraphy of ^{111}In-hMN-14 given in first and second injections or by measurement of radioactivity in pooled urine samples from patients who received second dose of ^{111}In-hMN-14 with ^{90}Y-hMN-14 therapy dose.

RESULTS

Adverse Events During Antibody Infusions

A total of 29 infusions of radiolabeled hMN-14 were administered (14 patients received 2 infusions and 1 patient received only 1 infusion). No patient was premedicated for allergic reactions before the antibody infusion, and no antibody infusion was cancelled because of an adverse event. Two patients experienced mild-to-moderate allergic-type reactions: redness, pruritus, periorbital hives, chills, and mild hypertension (from 100/80 mm Hg at baseline to 120/90 mm Hg after infusion) after the first antibody infusion. These 2 patients then received the therapy infusion without premedication and without complications.

Pharmacokinetics

The WB effective $t_{1/2}$ for the ^{111}In-hMN-14 IgG was 62.1 ± 3.2 h ($n = 15$), which indicates that only a small portion of the total radioactivity injected was cleared from the body. Urine collection indicated that between 13% and 19% of the total injected ^{111}In or ^{90}Y radioactivity was excreted over 7 d ($n = 2$; collection over only 3 d in 1 patient accounted for 7% of the total injected radioactivity). Although the radioactivity in the urine was not analyzed, the amount of radioactivity in the first 24 h represented nearly 90% of what was determined as nonantibody bound (i.e., chelated with DTPA) ^{111}In or ^{90}Y from the ITLC results on the starting radiolabeled product. Since the majority of a chelated radiometal was expected to excrete quickly, it is likely that the elimination fraction over the first 24 h was almost entirely due to the nonantibody–bound fraction in the injected product. External scintigraphy did not reveal any substantial uptake or movement of radioactivity through the GI tract and, thus, urinary excretion was the major route of elimination. As shown in Table 2, the WB effective $t_{1/2}$ measured for ^{90}Y-hMN-14 based on urine collection in these 3 patients corresponded well to the predicted values obtained from external scintigraphy of the ^{111}In-hMN-14 given in either the first or second injections as well as to the clearance of the ^{111}In-hMN-14 based on urine.

The blood clearance data (both the effective and estimated biologic) for the ^{111}In- and ^{90}Y-hMN-14 IgG were adequately defined by a monoexponential function in all patients. One patient (injection 1 in patient 1818; plasma CEA was 3,650 ng/mL) had a sharp decline in the amount of radioactivity in the first blood sample (40 min) to the second sample taken at 85 min (23.2 to 14.0 %ID/L [percentage injected dose per liter]), but the remaining 6 samples collected from 85 min to 143 h were fit well by a monoexponential function. The only other indication that plasma CEA might have been affecting early blood clearance was the observation that in the 3 patients with plasma CEA levels ≥1,800 ng/mL, only ~60% of the total injected dose was estimated in the total blood volume of the first sample taken with 1 h of the end of infusion, whereas >90% of the radioactivity could be accounted for in all other patients (i.e., plasma CEA ≤ 1,180 ng/mL). These data suggest that at higher plasma CEA concentrations, antigen-antibody complexes may have formed and were cleared from the blood by the time the first samples were collected. Size-exclusion HPLC showed no more than 15% of the radioactivity in a high-molecular-weight fraction when plasma CEA exceeded 1,000 ng/mL. Thus, the preinfusion of the unlabeled antibody before the radiolabeled antibody appeared to have minimized CEA-hMN-14 complex formation. Figure 2 shows the relationship between the predicted (based on the first ^{111}In-hMN-14 IgG) and observed (measured ^{90}Y-hMN-14) blood clearance of ^{90}Y-hMN-14 to that of the baseline plasma CEA. Plasma CEA was a significant contributing factor to the observed effective clearance $t_{1/2}$ but did not reach a statistically significant level for the predicted effective $t_{1/2}$ or the predicted or observed residence times. The proportion of variation that is explained by circulating CEA for each of these end points is relatively small (i.e., <35%).

The mean blood biologic half-life ($t_{1/2}$) for the ^{111}In-hMN-14 ($n = 15$) was 81.2 ± 24.0 h (range, 44.8–115.4 h),

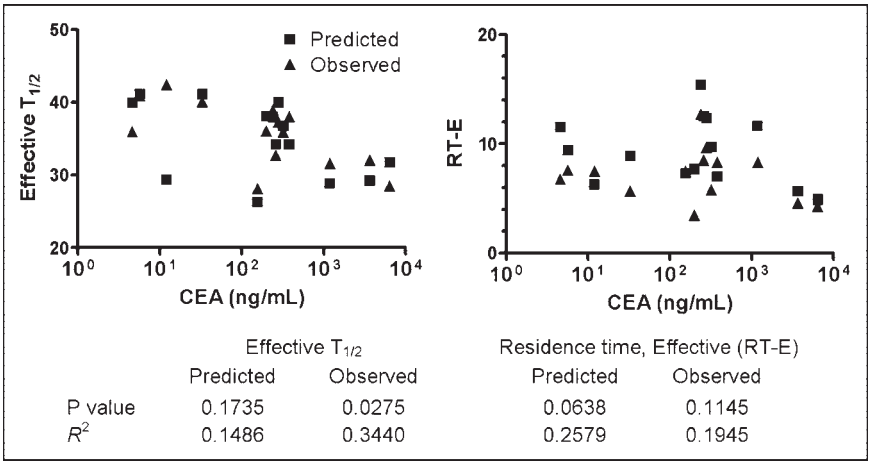

	Effective $T_{1/2}$		Residence time, Effective (RT-E)	
	Predicted	Observed	Predicted	Observed
P value	0.1735	0.0275	0.0638	0.1145
R^2	0.1486	0.3440	0.2579	0.1945

FIGURE 2. Impact of plasma CEA on blood pharmacokinetic behavior of ^{90}Y-hMN-14 IgG (observed) and that predicted for ^{90}Y-hMN-14 IgG from ^{111}In-hMN-14 IgG injection given 1 wk earlier (predicted).

whereas for the ^{90}Y-hMN-14 ($n = 14$) was 83.6 ± 22.9 h (range, 50.2–125.6 h), suggesting that both injections were cleared at a similar rate. Although a paired analysis of the effective half-lives of the predicted (from ^{111}In-hMN-14 injection 1) and measured ^{90}Y-hMN-14 from injection 2 were not significantly different (34.9 ± 5.1 h vs. 35.6 ± 4.5 h, respectively; $P = 0.546$), the predicted effective blood residence time for ^{90}Y-hMN-14 IgG based on the first ^{111}In-hMN-14 injection was significantly higher (9.3 ± 3.0 h/L; $n = 14$) than that measured for the ^{90}Y-hMN-14 in the second injection (7.2 ± 2.4 h/L; $P = 0.002$ for predicted vs. observed using a paired t test). These data suggest that if the red marrow dose for the ^{90}Y-hMN-14 were based on the blood clearance of ^{111}In-hMN-14 IgG given in the first injection, in many cases it would have been overestimated by about 20%. To further examine this issue, 3 patients were given a second injection of ^{111}In-hMN-14 IgG along with their ^{90}Y-hMN-14 therapy dose. Table 3 provides red marrow radiation-absorbed dose estimates by 4 different methods. The first method utilizes the blood and WB clearance from the direct measurement of ^{90}Y activity in the blood and urine of these patients after the ^{90}Y-hMN-14 IgG therapy dose and was considered the standard for comparison. Method 3 represents the use of a pretherapy study with ^{111}In-hMN-14 performed 1 wk in advance of the ^{90}Y-hMN-14 therapy study. In 2 of the 3 cases, this method overestimated the radiation-absorbed dose to the red marrow by nearly 35% when compared with the estimate provided by the directly measured ^{90}Y-hMN-14 IgG blood and urinary clearance data (method 1). Data generated from the clearance of the ^{111}In-hMN-14 coinjected with the ^{90}Y-hMN-14 (methods 2 and 4) more closely approximated the results found by direct measurement of the ^{90}Y activity. These data suggest that radiation dose estimates may be more reliably obtained from the ^{111}In-labeled antibody if it were coinjected with the ^{90}Y-labeled antibody. Using external scintigraphy of the sacrum or lumbar spine to derive red marrow dose may reduce some of this variability. For example, in 2 of the patients co-injected with ^{111}In-hMN-14, the red marrow dose for the first and second injections would be within 10% (e.g., 1.03 vs. 1.11 mGy/MBq and 2.70 vs. 2.97 mGy/MBq). The other patient had tumor involvement in the lumbar and sacral areas, preventing use of these regions for estimation of red marrow dose. Although this situation was not encountered frequently, it does illustrate the need to have alternate regions that could be used for external scintigraphy or reliable estimates provided from blood clearance data. Because radiation dose estimates can vary considerably when derived by different methods (i.e., imaging vs. blood clearance), it is important that the same method be used, particularly if the dosage assignment is to be based on red marrow dose estimates. For example, a review of the red marrow dose derived from blood clearance or external imaging of the ^{111}In-hMN-14 given in the first injection revealed that these estimates were within 25% of each other in 6 of 11 patients, but in 5 patients, the radiation dose derived from external scintigraphy was ≥50% higher compared with that derived from the blood clearance data (Fig. 3).

TABLE 3
Comparison of 4 Methods for Estimating Red Marrow Dose

Patient no.	Red marrow radiation-absorbed dose for ^{90}Y-hMN-14 IgG (mGy/MBq)			
	Method 1*	Method 2†	Method 3‡	Method 4§
1827	1.08	1.27	1.46	1.19
1831	1.14	1.16	1.03	1.08
1889	0.97	1.24	1.30	1.11

*Blood and urine clearance data of ^{90}Y-hMN-14 given in injection 2.
†Blood and urine clearance of ^{111}In-hMN-14 coadministered with ^{90}Y-hMN-14 (second injection).
‡Blood and WB (scintigraphy) clearance based on ^{111}In-hMN-14 given in first injection.
§Blood and WB (scintigraphy) clearance based on ^{111}In-hMN-14 given in second injection.

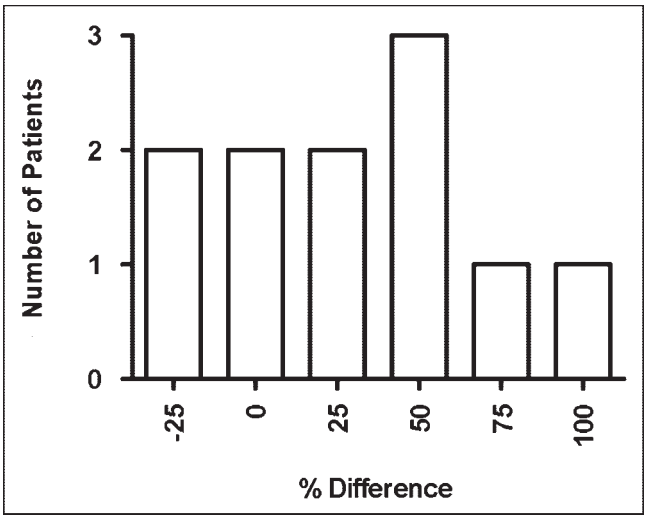

FIGURE 3. Frequency distribution shows number of patients for whom radiation-absorbed dose to red marrow (RM) by imaging was calculated to be lower (negative) or higher (positive) than dose derived from blood clearance data. Determination of RM dose by external scintigraphy was possible in 12 of 14 patients given ^{90}Y-hMN-14. Data from a 16-y-old subject were also not included in this analysis of adult patients. In this subject, dose derived from imaging study was 52.5% less than that derived from blood clearance data.

Biodistribution and Tumor Targeting

Table 4 summarizes the imaging sensitivity for the ^{111}In-hMN-14 IgG using CT as the standard comparator. A total of 156 lesions were documented by independent radiology review of the baseline CT. Seventy-nine of these lesions were noted in the bone of 3 patients. The ^{111}In-hMN-14 IgG identified 125 lesions (80% overall sensitivity; 78/79 of the bony lesions, for a sensitivity of 98.7%), but 16 additional lesions were documented on the ^{111}In-hMN-14 scan that were not seen even after further evaluation of the CT studies. Sensitivity was lowest in the lungs, but many of these lesions were ≤1.0 cm. Figure 4 shows the time course of WB images of a patient given 2 sequential injections of the ^{111}In-hMN-14 IgG to illustrate the similarity in targeting for both of these studies. This particular patient had diffuse nodular pulmonary disease, which was not seen on the ^{111}In-hMN-14 imaging study, but the multiple bony lesions were targeted and readily apparent within 24 h.

Organ and Tumor Dosimetry

Table 5 provides the average radiation-absorbed dose for the ^{111}In- and ^{90}Y-hMN-14 in several of the major organs. Since the 2 methods used in this trial for quantitation of radioactivity provide similar estimates for all organs except the lungs, the radiation-absorbed dose to the lungs is not included in Table 5. The average absorbed dose for ^{90}Y-hMN-14 to the lungs using the BFM was 2.78 ± 0.76 mGy/MBq (n = 8; range, 1.84–4.19 mGy/MBq), whereas for the MGMM it was 1.92 ± 0.32 mGy/MBq (n = 5; range, 1.57–2.24 mGy/MBq). The highest dose was delivered to liver and, since CEA-anti-CEA complexes would most likely be transported to the liver, an examination was made to determine if the radiation dose to the liver increased in patients with higher plasma CEA levels. Interestingly, there appeared to be a trend for the predicted absorbed dose to the liver to decrease as CEA increased (Fig. 5), but there was not a significant correlation between the liver dose and plasma CEA (P = 0.132; R^2 = 0.234), primarily due to the variability in absorbed dose to the liver observed between 100 and 1,000 ng/mL of circulating CEA. However, there was a significant correlation between the effective residence time in the blood and the liver dose (P = 0.002; R^2 = 0.671), indicating that as the concentration of radioactivity was sustained in the blood, the radiation-absorbed dose to the liver increased. The highest total dose delivered to the organs based on scintigraphy was 963, 2,175, 1,185, and 893 cGy to the red marrow, liver, kidneys, and lungs, respectively. Organ dosimetry derived from the coadministered ^{111}In-hMN-14 was generally within 10% of the first ^{111}In-hMN-14 injection (n = 3), suggesting that there was not a significant deviation in distribution and clearance of the radioactivity in the organs between the 2 injections.

Radiation-absorbed doses were calculated in 29 well-defined tumors in 8 patients, using the first ^{111}In-hMN-14 injection data. Nearly half of these lesions were in the bone (15/29, with 13 bony lesions in 1 patient). The first ROI generation for tumor dosimetry was possible in 24 of 29 lesions within 24 h, with 5 lesions being clearly delineated within 2–3 h. Interestingly, the maximum effective uptake occurred within 48–72 h in 24 lesions, which indicates that uptake occurred progressively over this time. In fact, the radioactivity concentration in the tumor, as determined from the first ROI to the ROI obtained at the maximum uptake, increased an average of 42% ± 44% (range, 0%–209%). The average estimated radiation dose delivered to the tumor in these 29 tumors was 15.1 ± 10.8 mGy/MBq (55.8 ± 39.8 cGy/mCi) (range, 1.51–47.1 mGy/MBq; median, 11.0 mGy/MBq). The average tumor-to-red marrow, tumor-to-liver, tumor-to-lungs, and tumor-to-kidneys ratios were 15.0 ± 11.0, 5.1 ± 3.6, 6.9 ± 6.1, and 9.0 ± 8.7, respectively. Figure 6A illustrates a trend for the lower radiation doses to tumors of larger size. It was possible to estimate doses to several very small tumors (e.g., ≤5 g) because of

TABLE 4
Targeting Sensitivity for ^{111}In-hMN-14 Based on CT

Region	No. of CT lesions	TP	FN	UP	Sensitivity (%)
Head/neck	26	21	5	5	80.8
Chest	68	47	21	8	69.1
Liver	15	12	3	1	80.0
Abdomen	21	19	2	1	90.5
Pelvis	26	26	0	1	100.0
Total	156	125	31	16	80.1

TP = true-positive; FN = false-negative; UP = unconfirmed positive.

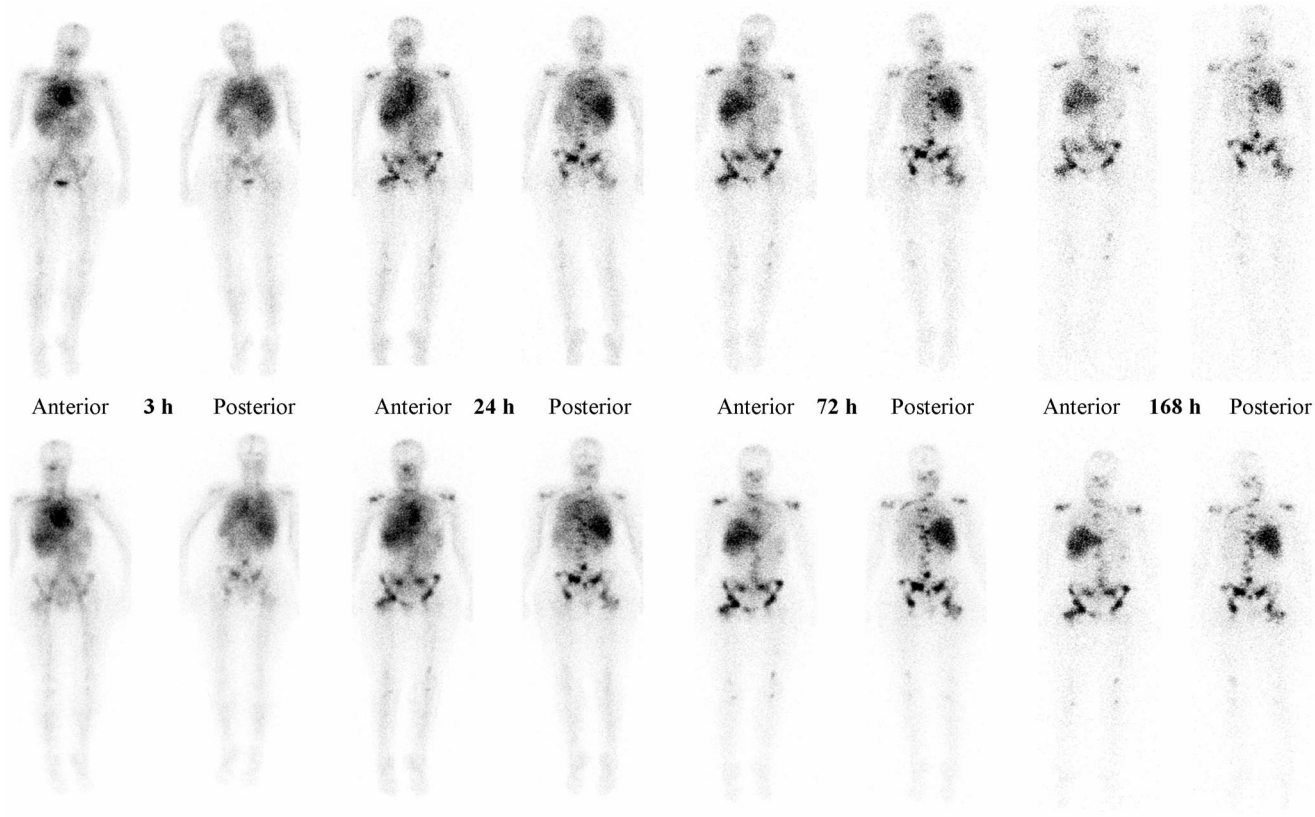

FIGURE 4. Anterior and posterior WB images of patient 1831 shows biodistribution of first injection of ^{111}In-hMN-14 IgG (top) and ^{111}In-hMN-14 IgG given with ^{90}Y-hMN-14 IgG injection 1 wk later (bottom).

the high contrast afforded by the uptake of the antibody, but also the anatomic positioning in less-vascularized regions of the body. Based on the total radioactivity injected, the majority of the tumors received >2,000 cGy, with 7 tumors, ranging in size from 0.7 to 33.5 g, receiving >5,000 cGy and with one 14.1-g bony lesion in the pelvis receiving 14,126 cGy (Fig. 6 B).

Dose Escalation and Toxicity

Enrollment started at a dose level of 740 MBq/m^2. PBSCs were reinfused in this group of patients within 7–8 d of the ^{90}Y treatment, and none of the patients developed grade 4 hematologic toxicity. PBSCs were reinfused in the 3 patients receiving 1,110 MBq/m^2 within 9–10 d. Two patients developed grade 4 leukopenia/neutropenia starting 10 and 13 d after the ^{90}Y-hMN-14 IgG, lasting up to 5 d. At the 1,480 MBq/m^2 dose, PBSCs were reinfused within 9–12 d, and only 1 patient developed grade 4 leukopenia (with only grade 3 neutropenia) starting 12 d after the ^{90}Y-hMN-14 IgG, which lasted 4 d. None of these 9 patients developed a nonhematologic DLT.

Escalation proceeded to 1,850 MBq/m^2, with the first 3 patients all developing grade 4 leukopenia/neutropenia that

TABLE 5
Organ Dosimetry Derived from External Scintigraphy of First ^{111}In-hMN-14 Injection

Dosimetry for	WB	RM	Liver	Kidneys	Spleen
^{111}In-hMN-14					
mGy/MBq	0.146 ± 0.016	0.208 ± 0.041	0.630 ± 0.168	0.330 ± 0.097	0.327 ± 0.095
Range	0.108–0.162	0.162–0.297	0.378–0.946	0.162–0.540	0.189–0.459
n	14	12	11	10	12
^{90}Y-hMN-14					
mGy/MBq	0.649 ± 0.081	1.65 ± 0.59	4.35 ± 1.32	2.65 ± 1.05	2.27 ± 0.89
Range	0.486–0.730	1.03–2.73	2.38–6.81	1.05–5.08	1.0–3.38
n	13	11	11	10	12

Organs involved with tumor or having underlying or overlying tumor were not measured.

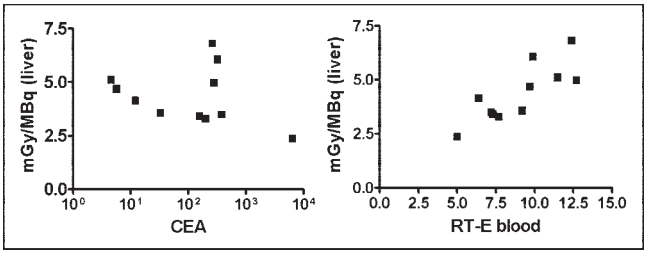

FIGURE 5. Potential factors contributing to radiation-absorbed dose to liver. RT-E = residence time, effective.

lasted for up to 9 d, and 1 patient developing grade 4 thrombocytopenia lasting 1 d. PBSCs were reinfused in these patients within 10–12 d of treatment. One of these patients developed grade 4 cardiac toxicity manifested by cardiac tamponade, which required hospitalization and surgery. This patient had a moderate pericardial effusion and significant metastatic mediastinal lymphadenopathy at the baseline CT scans, which may have contributed to this toxicity. Therefore, the protocol was amended to exclude such patients, but only 2 patients were enrolled before closing the trial. One patient developed grade 4 leukopenia/neutropenia that lasted for up to 13 d and grade 4 thrombocytopenia lasting 1 d, but this patient also developed grade 4 shortness of breath and pneumonitis requiring long-term intubation and subsequently tracheostomy. Further analysis by independent medical reviewers of the conditions that led to the grade 4 respiratory toxicity in this patient revealed that multiple factors likely caused this toxicity, including infection, fluid overload, and the possibility that the patient had a central respiratory depression before intubation, secondary to significant doses of narcotics and hypnotics given to control pain. There was no clinical evidence to suggest that he developed radiation pneumonitis that contributed to his respiratory failure, and based on the ^{111}In-hMN-14 imaging study, the radiation-absorbed dose to the lungs for the ^{90}Y-hMN-14 dose administered was only 799 cGy. Nevertheless, with 2 patients treated at the 1,850 MBq/m^2 dose level experiencing DLT complications, further enrollment at this dose level was terminated. Thus, the trial was terminated with 1,480 MBq/m^2 of ^{90}Y-hMN-14 IgG when followed 24 h by Dox at the dose used in this protocol declared as the MTD.

Table 6 lists all nonhematologic adverse events recorded during the course of this trial, although several of these were not considered related to the treatment regimen. Many of these toxicities are commonly observed with Dox alone but, because of limited clinical experience with ^{90}Y-hMN-14 IgG, particularly at doses ≥1,110 MBq/m^2, it is not possible to gauge the incidence or severity that might be attributed solely to the ^{90}Y-hMN-14 IgG or the extent by which the combination affected the incidence or severity.

The most frequent nonhematologic toxicity observed was GI (n = 14) in the form of nausea (n = 13), vomiting (n = 9), and diarrhea (n = 10). All of these events were transient, with complete recovery in <2 wk, except in 1 patient who continued to have grade 2 vomiting for 19 d and grade 2 nausea for 63 d. There was no correlation between the administered radioactivity and the occurrence, severity, or duration of GI toxicity. Other nonhematologic toxicities included transient grade 1 hepatic toxicity in 3 patients, manifested by transient elevation in liver enzymes. Seven patients experienced grade 1 to grade 2 pulmonary toxicity and another patient had grade 4 pneumonitis that was considered DLT. The grade 1 (n = 2) and grade 2 (n = 5) pulmonary toxicities were manifested by decreases in the forced expiratory volume and/or DLCO (n = 3), or by mild/moderate shortness of breath (n = 4). Eight patients had cardiac toxicities. Four patients had grade 1 or grade 2 asymptomatic decreases in the left vertricular ejection fraction on the follow-up MUGA scan performed at 2–7 mo after treatment. One patient complained of palpitations 1 y after treatment, and another had atrial fibrillation or flutter 5 mo after treatment. A third patient was diagnosed with pleuropericarditis 3 mo after treatment when he was noted to have pericardial rub on cardiac auscultation. The other 2 cardiac events were considered DLTs and were described earlier.

In summary, the hematologic toxicities were moderate to severe, but with the aid of stem cells, all patients engrafted and recovered their blood counts to normal levels within 8–39 d. Cardiopulmonary toxicity was dose limiting at 1,850 MBq/m^2 and, because of the low incidence of severe

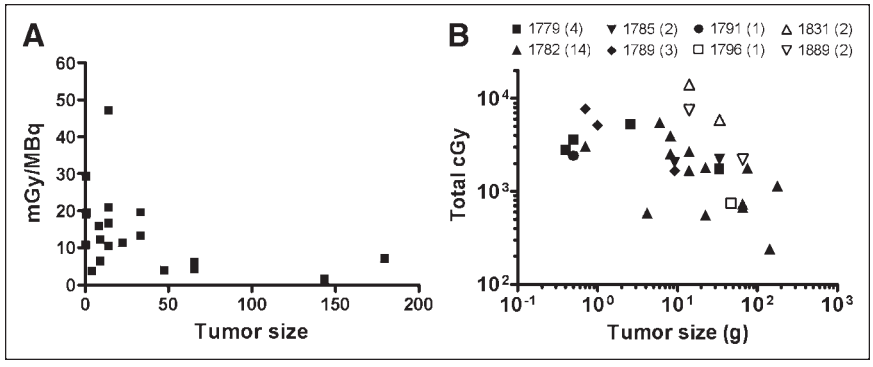

FIGURE 6. Tumor dosimetry shows distribution of radiation-absorbed dose delivered either on a per MBq basis (A) or total dose (B) based on size of tumor. B also lists total dose in each of 8 patients (4-digit patient numbers) and number of lesions per patient in parentheses.

TABLE 6
Occurrence and Severity of All Nonhematologic Adverse Events

Dose level	*n*	Adverse event	Grade 1/2	Grade 3/4
740 MBq/m^2	3	GI	3	0
		Pulmonary	1	0
		Cardiac	2	0
1,110 MBq/m^2	3	GI	2	1
		Pulmonary	2	0
		Cardiac	2	0
		Neurologic	1	0
1,480 MBq/m^2	3	GI	2	1
		Pulmonary	3	0
		Cardiac	2	0
		Neurologic	1	0
1,850 MBq/m^2	5	GI	5	0
		Pulmonary	1	1
		Cardiac	0	2
		Hepatic	2	0
		Renal	1	0
		Neurologic	0	1

toxicities at 1,480 MBq/m^2, it was chosen as the MTD for this treatment regimen.

HAHA

None of the 15 patients enrolled in the study was positive for HAHA before receiving the first infusion of hMN-14 IgG. Of the 14 patients who received treatment, 13 had at least 8 wk or more follow-up testing, whereas the other patient had testing available for only 4 wk after infusion. Four patients developed a detectable level of HAHA within 8–12 wk of infusion. Three of these met the criteria to be positive by the HPLC assay (*29*). The other patient was tested by the ELISA method and had a value of 727 ng/mL at week 12. The duration of these responses was not determined.

Antitumor Response

Of the 14 patients who received therapy, one patient was not assessable for tumor response, and another 7 patients showed disease progression on the follow-up CT scans, even though some of these patients had decreases or stabilization of tumor markers for a brief period of time before progressing. Four patients had stable disease on CT scans for 3, 3.5, 6, and 8.5+ mo. All of these patients also had stable tumor markers for at least the duration of the stabilization of the disease on CT scan. Two patients, patients 1779 and 1785, both treated at 740 MBq/m^2, had minor responses for 27+ and 10 mo, respectively. Circulating tumor markers (calcitonin or CEA) in these 2 patients were also stable for 12 and 10 mo, respectively. One patient (patient 1853), treated at 1,850 MBq/m^2, presented with multiple lesions in the neck, chest, and liver. Several index lesions decreased by >25% and the serum calcitonin level decreased by 55% (13,118 to 5,900 pg/mL) 1 mo after treatment, with a 62% overall reduction at 3 mo. The initial radiology review suggested that new lesions may have developed at 1 mo, indicating progression, but subsequent review by 3 other radiologists and an oncologist concluded that there were no new lesions and that there was a 68% overall reduction in tumor mass. Since there was no follow-up confirmatory CT scan, this was scored as an unconfirmed partial response. However, follow-up 4 mo after treatment indicated calcitonin and CEA levels had decreased 77% and 60%, respectively, but thereafter they began to increase, and medical notes indicated that the patient had progressed and ultimately died 8 mo after treatment. Figure 7 illustrates the response seen in 2 of the index lesions that were located in the liver. Other lesions in the neck and chest also had similarly significant decreases in their size.

Dosimetry estimated 2,916 cGy was delivered to the larger (estimated mass size = 234 g) tumor mass in the liver of this patient. The index lesion in the upper portion of the liver was not readily identifiable on planar views and, therefore, radiation-absorbed doses were not determined. In the other patients with soft-tissue masses for whom dosimetry was obtained, there was no trend for lesions receiving higher doses to have any greater evidence of stabilization or reduction in size than those receiving lower doses. Many lesions that were amenable for dosimetry determinations were in the bone, but measures were not taken to assess response of these lesions.

DISCUSSION

Although it is a relatively rare disease, MTC has an unmet medical need due to the lack of effective therapeutic options after failing surgery. Several new therapeutic modalities are being examined (*30*), including radionuclides (*31*), gene therapy (*32*), and immunotherapy (*33*). MTC produces several unique markers that could be used for highly selective delivery of therapeutic modalities. Although calcitonin is the most highly specific marker, being produced only by the C cells of this cancer type, other tumor markers, such as the somatostatin receptor and CEA, are also commonly produced by MTC. Our group, as well as others, have shown that antibodies to CEA target MTC very well and, therefore, we have focused on the use of radiolabeled anti-CEA antibodies as a potential treatment for MTC (*12–15*).

Several other clinical trials have examined the treatment of MTC using either an ^{131}I-anti-CEA antibody or an ^{131}I-labeled peptide pretargeted by a bispecific anti-CEA antibody (*16,17,34,35*). Excellent targeting was reported in each of these phase I/II trials but, for the most part, only a few minor responses and disease stabilization were reported. One of these trials used high-dose radioimmunotherapy (RAIT) with an ^{131}I-labeled murine anti-CEA F(ab)$_2$ in conjunction with PBSC rescue, in which one patient experienced a partial response for 1 y after receiving 15.36 GBq of the radioiodinated antibody with the delivery of 5,000, to as much as 73,000 cGy to multiple lesions in the

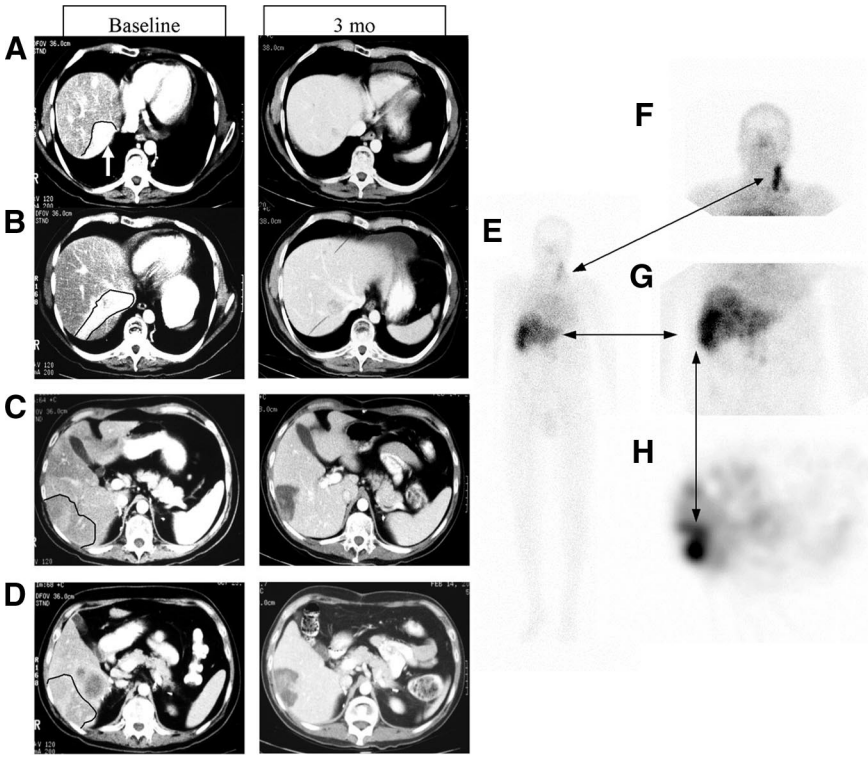

FIGURE 7. Patient 1853, a 41-y-old man, presented with widely metastatic MTC in neck, chest, and liver and was treated at a dose of 1,850 MBq/m^2 with ^{90}Y-hMN-14 IgG + 60 mg/m^2 Dox 1 d later. Two index lesions selected in baseline CT images were in liver. (A and B) Sequential slices that show 1 index lesion as an irregularly shaped tumor in upper portion of left lobe of liver. (C and D) Two slices though lower portion of liver show another very large laterally positioned lesion that was apparent in 11 consecutive 7.0-mm slices. Extent of this lateral lesion can be better appreciated in nuclear images to the right, where its size was estimated to be 234 g. Regions are drawn around baseline lesions, since several tumors were poorly enhanced. Three-month CT scan shows considerable reduction in upper lesion with noticeable reduction and more necrosis in lateral lesion. WB and anterior planar nuclear images (E and G, respectively) taken 6 d after ^{111}In-hMN-14 IgG show very high accretion of radioactivity in lateral liver lesion as well as uptake in several other locations throughout liver. (H) Transaxial SPECT view of liver at 48 h also shows intense uptake in lateral lesion. (F) Antibody targeting of what proved to be 5 separate lesions in neck, with a sum of the product of their perpendicular diameters at baseline equaling 9.64 cm^2, decreasing to a sum of 3.28 cm^2 at 3 mo (66% reduction).

liver (*17*). In addition, disease stabilization was seen in 10 of 12 patients for 1–16 mo, and a minor response for 3 mo was observed in another patient. These results were encouraging, but high doses of ^{131}I requiring extended hospitalization lead us to examine ^{90}Y-labeled anti-CEA antibody as an alternative, since ^{90}Y could be given on an outpatient basis. In addition, ^{90}Y was considered to have an advantage for treating the large-sized lesions that are typically seen in patients with extensive metastatic disease. Furthermore, data in animal models for MTC suggested that therapeutic responses might be improved with the addition of Dox (*20–22*); thus, a trial was designed to combine a single dose (i.e., 60 mg/m^2) of Dox with the ^{90}Y-hMN-14 IgG. Finally, because RAIT of advanced solid tumors in a nonmyeloablative setting has not been promising, this trial was also designed to use PBSCs to reduce the risk of dose-limiting myelotoxicity and allow for higher doses of radioactivity to be administered. Indeed, in a pretargeting therapy trial in patients with CEA-producing tumors, Kraeber-Bodéré et al. (*35*) reported that patients with MTC were more likely to experience more severe myelosuppression than patients with other CEA-producing tumors, suggesting that there is early spread to the bone marrow that might not be readily apparent with conventional detection methods. A retrospective analysis of MTC patients using MRI and immunoscintigraphy suggested that the incidence of bone marrow involvement is considerably higher than that which is usually reported for this disease (*36*). This suggests that red marrow dosimetry based on scintigraphic measurements would be preferred for MTC when diffuse bone marrow uptake is observed, particularly in a nonmyeloablative setting. PBSCs and G-CSF were used in this trial, and there was no evidence of more extensive hematologic toxicity or recovery time in patients with known bone marrow involvement than those without involvement.

As expected, tumor targeting with the radiolabeled anti-CEA IgG was excellent, with an overall sensitivity of >80% (98% for bony lesions). Although lesions in the liver were seen previously using ^{131}I-anti-CEA antibody, it was uncertain whether liver metastases would be seen with the ^{111}In-labeled antibody. The trial was designed to preinfuse additional unconjugated, nonradiolabeled anti-CEA IgG before infusion of the radiolabeled antibody in an attempt to reduce the possibility for elevated liver accretion of the radiolabeled antibody due to CEA–anti-CEA complexes. The relative success of this approach in reducing liver accretion could not be ascertained directly, since we have not performed similar studies without a preinjection of the unconjugated ^{111}In-hMN-14 IgG in patients with plasma CEA as highly elevated as in some of these patients. Although there was some indication in the patients with circulating CEA exceeding 1,800 ng/mL that CEA–anti-CEA complexes might have formed and cleared the blood by the time the first blood sampling occurred in this trial, there was

no evidence that these patients had increased radiation-absorbed doses to the liver. Size-exclusion HPLC of the plasma taken 1 h after the end of the radiolabeled antibody infusion revealed <15% of the radiolabeled antibody to be in the form of CEA-antibody complexes. The amount of complex formation seen in the 1-h sample was almost identical to that seen at 24 h, another indication that the amount of unlabeled antibody administered was sufficient to reduce the formation of these complexes. Thus, although the trial did not determine an optimal dose for the unconjugated antibody or whether a preinfusion (vs. a coinfusion) is required, the approach clearly allowed the elucidation of lesion targeting in the liver, and tumor dosimetry indicated that many tumors received >2,000 cGy, further suggesting that it was unlikely the additional unlabeled protein diminished the uptake of the radiolabeled antibody in the tumors. Ultimately, clinical trials with radiolabeled antibodies must focus on patients with less tumor burden than those enrolled in this study and, in this regard, the level of circulating plasma CEA would be expected to be considerably lower than 1,000 ng/mL, which might allow for lower administered antibody doses.

At the dose levels tested, no organ received more than the planned maximum allowable dose and, except for 1 case of cardiac toxicity, the radiation delivered to the critical organs did not result in severe toxicities. Radiation-absorbed dose to the heart wall, based on blood clearance data and assuming 10% of the blood radioactivity concentration was in the heart, was estimated to be 826 cGy in this patient. Using this same method to estimate absorbed doses to the heart wall, the other patients treated at the 1,850 MBq/m^2 dose level received between 568 and 1,200 cGy; thus, the radiation-absorbed dose calculated in this manner was not a useful predictor in this case. As an additional precaution though, the protocol was modified to exclude patients with extensive disease in the mediastinum and a pericardial effusion. Despite this precaution, escalation was terminated at 1,850 MBq/m^2 due to a second patient experiencing dose-limiting pulmonary toxicity with additional cardiac complications (heart wall dose estimated to be 1,127 cGy). Although the treatment was believed to be a major contributor to this second patient's cardiopulmonary toxicity, other factors were also thought to be involved. It is noteworthy that severe cardiopulmonary toxicity did not occur in non-Hodgkin's lymphoma patients given myeloablative doses of an ^{131}I-labeled anti-CD20 antibody until the radiation dose to the lungs exceeded 2,000 cGy (*37*). Thus, despite receiving only ~800 cGy to the lungs, since the severe pulmonary toxicity experienced by this patient was the second dose-limiting event at the 1,850 MBq/m^2 dose level, the trial was terminated, and 1,480 MBq/m^2 was declared as the MTD for this treatment combination. It is not clear what role Dox, which has a well-known cardiac toxicity (*38*), played in the development of DLT in these 2 patients. Although there is no clinical experience with ^{90}Y-hMN-14 IgG alone at comparable doses, the prior clinical trial using high-dose ^{131}I-murine anti-CEA F(ab)$_2$ also reported 2 cases of grade 2 cardiac toxicities and 4 cases of grade 1 pulmonary toxicities, as well as mild-to-moderate GI toxicity in 7 of 12 patients and 1 case of grade 3 GI toxicity (*17*). Hematologic toxicity was well controlled with PBSCs, with engraftment occurring readily in all patients, even with radiation-absorbed doses to the red marrow estimated to be as high as 960 cGy. Our prior experience in nonmyeloablative RAIT trials indicated that hematologic toxicity nadirs could occur within 4 wk of treatment; thus, the trial was designed to ensure that PBSCs were reinfused within 2 wk of the ^{90}Y-hMN-14 treatment in an attempt to forestall the development of severe toxicities for extended periods. The hematologic data indicated that this procedure was effective in ensuring engraftment and reducing the period during which patients experienced severe toxicity with doses as high as 1,850 MBq/m^2 of the ^{90}Y-IgG. Finally, it is important to note that allergic reactions were relatively infrequent (2/29 infusions), even without premedicating patients.

In comparison with the dosimetry reported for other ^{90}Y-labeled antibodies, where radiation-absorbed doses to the tumor were infrequently >2,000 cGy (*38–40*), the targeting potential of the ^{90}Y-anti-CEA IgG in MTC was very promising, with a majority of the lesions amenable for dosimetry determinations receiving >2,000 cGy and with others receiving ≥5,000 cGy. Had everyone treated on this trial received 1,480 MBq/m^2, >5,000 cGy would have been delivered to 12 of 29 (41%) lesions, with 4 lesions receiving >10,000 cGy, which may have improved the response rate. Several lesions that had dosimetry assessments were bone metastases, which were not assessed for response. Three soft-tissue tumors that had dosimetry determinations and responded to treatment decreased in size by about 40% with the delivery of about 2,000 cGy. However, there were 7 lesions that received >2,000 cGy that were stable or decreased by ≤20% for 1–6 mo. Despite these observations to individual lesions, overall there was only 1 patient in whom the total disease burden decreased by >50%, with the largest lesion in the liver receiving ~2,900 cGy. These observations indicate that the treatment regimen had some effect but, in many of these patients, the disease was too advanced for the therapy to be more active. Clearly, this treatment should focus more on patients with less advanced disease. Since an elevated calcitonin level is considered to be an excellent indicator of even occult MTC, future trials may consider an earlier intervention with RAIT and use this tumor marker in combination with an extended period of observation in order to evaluate treatment response. Calcitonin and CEA levels were observed in several of these patients to decrease after treatment, even patients in whom the disease subsequently progressed by CT. However, this trial did not provide any further conclusions on the use of these markers to monitor response to RAIT.

This study is among a relatively small number of clinical trials that have combined radiolabeled antibodies with standard chemotherapeutic agents (e.g., 5-flurouracil or pacli-

taxel) in an attempt to enhance the therapeutic activity of radiolabeled antibodies in solid tumors (*41,42*). Whereas in these other approaches, in which the dose of the radiolabeled antibody used in the combination could not be escalated beyond the dose-limiting hematologic toxicity, in this trial, the use of PBSCs allowed the ^{90}Y-hMN-14 IgG dose to be escalated beyond what has typically been reported for other ^{90}Y-labeled antibodies without the aid of PBSC rescue. Previous studies in non-Hodgkin's lymphoma using an ^{131}I-labeled anti-CD20 antibody that was escalated with the aid of PBSC rescue determined that cardiopulmonary toxicity was dose limiting (*43*). Thus, in our trial, Dox represented a treatment modality that would likely have overlapping toxicity and, therefore, it is worth asking whether the addition of Dox to this treatment regimen was useful or merely a source of additional toxicity that curtailed further escalation of the ^{90}Y-hMN-14. In animal studies suggesting that the addition of Dox to a RAIT treatment is synergistic (*20–22*), the mice were given a single Dox injection that itself was near a lethal dose, but this was limited by hematologic toxicity. In the report by Stein et al. (*21*), this dose was determined to be 60 mg/m^2 (216 μg), similar to the 200-μg dose reported by Behr et al. (*20*), and this provided the rationale to test a single Dox dosage of 60 mg/m^2 in this trial. This amount of Dox can be therapeutic, but it commonly is followed every few weeks with sequential doses of equal magnitude, ultimately being limited by a cumulative dose of 300–500 mg/m^2 to reduce the risk of severe cardiotoxicity. Thus, whereas the amount of Dox given in this trial alone would not be expected to elicit severe cardiac toxicity, the impact of this combination on cardiotoxicity is unknown. Importantly, too, although the amount of Dox given was the same in animals and patients, it is uncertain whether this dose in patients was sufficient to achieve a level required for optimal synergy of the 2 agents, as seen in mice. Thus, the future examination of combinational approaches would greatly benefit by having a more objective measure of parameters required to optimize the treatment, both in terms of toxicity and efficacy. Determination of the DLT and MTD for the ^{90}Y-hMN-14 IgG alone with and without PBSC support in MTC also would be important, so that the additive toxicity profile and potential efficacy of a combination can be understood better. Though there was a second arm open at the same time that would have enrolled patients who had a prior exposure to Dox with escalating doses of ^{90}Y-hMN-14 alone using PBSCs, only 1 patient referred to this program had prior exposure to Dox, and thus this other cohort was not studied. We also note that other chemotherapeutic agents used clinically in the treatment of MTC, such as dimethyltriazenyl imidazole carboxamide (dacarbazine [DTIC]) (*22*), have been shown to augment the antitumor response in combination with ^{90}Y-hMN14 even more than Dox. DTIC's primary toxicity is hematologic and, therefore, with hematologic support, this may be a better agent to use in combination with ^{90}Y-hMN-14.

CONCLUSION

Although there was some promising evidence for antitumor activity, objective responses in this advanced disease population were rarely seen with this treatment regimen. This suggests that, similar to the clinical experience with radiolabeled antibodies in other solid tumors, they should be considered for use primarily in patients with less advanced disease. MTC is an excellent indication to test this hypothesis because of the specificity and sensitivity of several tumor markers in this disease. However, in considering the treatment of less advanced disease, and given the long survival time for surgically resected, locoregional disease, it is unlikely that PBSC support would be considered. Thus, new methods that have the capability of delivering higher radiation doses to tumors without resorting to hematologic support could provide the next generation of radionuclide-targeting strategies. In this regard, pretargeting approaches have been described that have been shown in preclinical models to be more effective than directly radiolabeled antibodies (*44–46*). A bispecific antibody pretargeting approach based on an anti-CEA antibody has shown excellent targeting and therapeutic prospects for ^{131}I- and ^{90}Y-labeled compounds that provide higher tumor-to-critical organ ratios in preclinical studies (*45,47*), and clinically (*35*), than the directly labeled antibody. Although a prior report of a study of 51 patients with persistently elevated calcitonin levels after initial surgery did not show a significant impact of local irradiation on the 10-y survival rate, the fact that there was evidence of a significant impact on the local relapse rate (*48*) encourages us to speculate that a regimen combining external-beam therapy (local control) with some form of RAIT with or without a chemotherapy regimen (systemic control) in patients with persistently elevated calcitonin levels could lead to the improved survival of these patients. Thus, developing a more successful treatment regimen for MTC remains a challenge, but RAIT continues to have a potential role.

ACKNOWLEDGMENTS

We thank the following individuals who made various contributions to the clinical studies and assessments: Douglas Dunlap; Sylvia Gargiulo; Thomas Herskovic, MD; Tom Jackson; Malik Juweid, MD; Joseph Lowry, MD; Clara Machado, MD; George Mardirrosian, PhD; Jeffrey Plutchok, MD; Jonathan Scheiner, MD; Lawrence Swayne, MD; and Stephen P. Toder, MD. We are particularly grateful to scientists and other staff at Immunomedics, Inc., for providing the antibody for our use, to the referring physicians for following their patients after treatment, and, most importantly, to the patients who participated. This study was supported in part by grant FD-R-001555-01 from the Food and Drug Administration and by Public Health Service grant CA79857 from the National Cancer Institute. David M. Goldenberg has a financial interest in Immunomedics, Inc., which supplied the antibody used in this study.

REFERENCES

1. Robbins J, Merino MJ, Boice JD Jr, et al. Thyroid cancer: a lethal endocrine neoplasm. *Ann Intern Med.* 1991;115:133–147.
2. Kebebew E, Ituarte PH, Siperstein AE, Duh QY, Clark OH. Medullary thyroid carcinoma: clinical characteristics, treatment, prognostic factors, and a comparison of staging systems. *Cancer.* 2000;88:1139–1148.
3. Brierley J, Tsang R, Simpson WJ, Gospodarowicz M, Sutcliffe S, Panzarella T. Medullary thyroid cancer: analyses of survival and prognostic factors and the role of radiation therapy in local control. *Thyroid.* 1996;6:305–310.
4. Nocera M, Baudin E, Pellegriti G, Cailleux AF, Mechelany-Corone C, Schlumberger M. Treatment of advanced medullary thyroid cancer with an alternating combination of doxorubicin-streptozocin and 5 FU-dacarbazine: Groupe d'Etude des Tumeurs a Calcitonine (GETC). *Br J Cancer.* 2000;83:715–718.
5. Orlandi F, Caraci P, Berruti A, et al. Chemotherapy with dacarbazine and 5-fluorouracil in advanced medullary thyroid cancer. *Ann Oncol.* 1994;5:763–765.
6. Wu LT, Averbuch SD, Ball DW, de Bustros A, Baylin SB, McGuire WP. Treatment of advanced medullary thyroid carcinoma with a combination of cyclophosphamide, vincristine, and dacarbazine. *Cancer.* 1994;73:432–436.
7. Shimaoka K, Schoenfeld DA, DeWys WD, Creech RH, DeConti R. A randomized trial of doxorubicin versus doxorubicin plus cisplatin in patients with advanced thyroid carcinoma. *Cancer.* 1985;56:2155–2160.
8. Porter AT, Ostrowski MJ. Medullary carcinoma of the thyroid treated by low-dose adriamycin. *Br J Clin Pract.* 1990;44:517–518.
9. Petursson SR. Metastatic medullary thyroid carcinoma: complete response to combination chemotherapy with dacarbazine and 5-fluorouracil. *Cancer.* 1988; 62:1899–1903.
10. Bonner JA, Lawrence TS. Doxorubicin decreases the repair of radiation-induced DNA damage. *Int J Radiat Biol.* 1990;57:55–64.
11. Mendelsohn G, Wells SA Jr, Baylin SB. Relationship of tissue carcinoembryonic antigen and calcitonin to tumor virulence in medullary thyroid carcinoma: an immunohistochemical study in early, localized, and virulent disseminated stages of disease. *Cancer.* 1984;54:657–662.
12. Juweid M, Sharkey RM, Behr T, et al. Improved detection of medullary thyroid carcinoma with radiolabeled antibodies to carcinoembryonic antigen. *J Clin Oncol.* 1996;14:1209–1217.
13. Juweid ME, Sharkey RM, Behr T, et al. Targeting and initial radioimmunotherapy of medullary thyroid carcinoma with I-131-labeled monoclonal antibodies to carcinoembryonic antigen. *Cancer Res.* 1995;55:5946–5951.
14. Vuillez JP, Peltier P, Caravel JP, Chetanneau A, Saccavini JC, Chatal JF. Immunoscintigraphy using ^{111}In-labeled F(ab′)$_2$ fragments of anticarcinoembryonic antigen monoclonal antibody for detecting recurrences of medullary thyroid carcinoma. *J Clin Endocrinol Metab.* 1992;74:157–163.
15. Peltier P, Curtet C, Chatal JF, et al. Radioimmunodetection of medullary thyroid cancer using a bispecific anti-CEA/anti-indium-DTPA antibody and an indium-111-labeled DTPA dimer. *J Nucl Med.* 1993;34:1267–1273.
16. Juweid ME, Hajjar G, Swayne LC, et al. Phase I/II trial of ^{131}I-MN-14 F(ab)$_2$ anti-carcinoembryonic antigen monoclonal antibody in the treatment of patients with metastatic medullary thyroid carcinoma. *Cancer.* 1999;85:1828–1842.
17. Juweid ME, Hajjar G, Stein R, et al. Initial experience with high-dose radioimmunotherapy of metastatic medullary thyroid cancer using ^{131}I-MN-14 F(ab)$_2$ anti-carcinoembryonic antigen (CEA) monoclonal antibody and autologous hematopoietic stem cell rescue (AHSCR). *J Nucl Med.* 2000;41:93–103.
18. Sharkey RM, Juweid M, Shevitz J, et al. Evaluation of a CDR-grafted (humanized) anti-carcinoembryonic antigen (CEA) monoclonal antibody in preclinical and clinical studies. *Cancer Res.* 1995;55:5935s–5945s.
19. Griffiths GL, Govindan SV, Sharkey RM, Fisher DR, Goldenberg DM. ^{90}Y-DOTA-hLL2: an agent for radioimmunotherapy of non-Hodgkin's lymphoma. *J Nucl Med.* 2003;44:77–84.
20. Behr TM, Wulst E, Radetzky S, et al. Improved treatment of medullary thyroid cancer in a nude mouse model by combined radioimmunochemotherapy: doxorubicin potentiates the therapeutic efficacy of radiolabeled antibodies in a radioresistant tumor type. *Cancer Res.* 1997;57:5309–5319.
21. Stein R, Juweid M, Zhang C-H, Goldenberg DM. Assessment of combined radioimmunotherapy and chemotherapy for treatment of medullary thyroid cancer. *Clin Cancer Res.* 1999;5(suppl):3199s–3206s.
22. Stein R, Chen S, Reed L, Richel H, Goldenberg DM. Combining radioimmunotherapy and chemotherapy for treatment of medullary thyroid carcinoma: effectiveness of dacarbazine. *Cancer.* 2002;94:51–61.
23. Sgouros G. Bone marrow dosimetry for radioimmunotherapy: theoretical considerations. *J Nucl Med.* 1993;34:689–694.
24. Siegel JA, Wu RK, Maurer AH. The buildup factor: effects of scatter on absolute volume determination. *J Nucl Med.* 1985;26:390–394.
25. Doherty P, Schwinger R, King M, et al. Distribution and dosimetry of indium-111 labeled F(ab′)$_2$ fragments in humans. In: Schlafke-Stelson A, Watson EE eds. *Proceedings of the Fourth International Radiopharmaceutical Dosimetry Conference.* Oak Ridge, TN: Oak Ridge Associated Universities; 1985:464–476.
26. Yeldell D, Mardirrosian G, Sharkey RM, Goldenberg DM. Comparison of the modified geometric mean and buildup factor internal dosimetry techniques used for organ activity quantitation of ^{131}I- and ^{90}Y-labeled antibodies [abstract]. *J Nucl Med.* 2001;42(suppl):22P.
27. Stabin MG. MIRDOSE: personal computer software for internal dose assessment in nuclear medicine. *J Nucl Med.* 1996;37:538–546.
28. International Commission on Radiological Protection. *Report of the Task Group on Reference Man.* ICRP Publication 23. New York, NY: Pergamon Press; 1975.
29. Hajjar G, Sharkey RM, Burton J, et al. Phase I radioimmunotherapy trial with iodine-131-labeled humanized MN-14 anti-carcinoembryonic antigen monoclonal antibody in patients with metastatic gastrointestinal and colorectal cancer. *Clin Colorectal Cancer.* 2002;2:31–42.
30. Moley JF. Medullary thyroid carcinoma. *Curr Treat Options Oncol.* 2003;4:339–347.
31. Bodei L, Handkiewicz-Junak D, Grana C, et al. Receptor radionuclide therapy with ^{90}Y-DOTATOC in patients with medullary thyroid carcinomas. *Cancer Biother Radiopharm.* 2004;19:65–71.
32. Drosten M, Putzer BM. Gene therapeutic approaches for medullary thyroid carcinoma treatment. *J Mol Med.* 2003;81:411–419.
33. Schott M, Feldkamp J, Klucken M, Kobbe G, Scherbaum WA, Seissler J. Calcitonin-specific antitumor immunity in medullary thyroid carcinoma following dendritic cell vaccination. *Cancer Immunol Immunother.* 2002;51:663–668.
34. Kraeber-Bodere F, Bardet S, Hoefnagel CA, et al. Radioimmunotherapy in medullary thyroid cancer using bispecific antibody and iodine 131-labeled bivalent hapten: preliminary results of a phase I/II clinical trial. *Clin Cancer Res.* 1999;5(suppl):3190s–3198s.
35. Kraeber-Bodéré F, Faivre-Chauvet A, Ferrer L, et al. Pharmacokinetics and dosimetry studies for optimization of anti-carcinoembryonic antigen x anti-hapten bispecific antibody-mediated pretargeting of iodine-131-labeled hapten in a phase I radioimmunotherapy trial. *Clin Cancer Res.* 2003;9(Pt 2):3973S–3981S.
36. Mirallié E, Vuillez JP, Bardet S, et al. High frequency of bone marrow involvement in advanced medullary thyroid cancer. *J Clin Endocrinol Metab.* 2005;90:779–788.
37. Minotti G, Menna P, Salvatorelli E, Cairo G, Gianni L. Anthracyclines: molecular advances and pharmacologic developments in antitumor activity and cardiotoxicity. *Pharmacol Rev.* 2004;56:185–229.
38. Tempero M, Leichner P, Baranowska-Kortylewicz J, et al. High-dose therapy with ^{90}yttrium-labeled monoclonal antibody CC49: a phase I trial. *Clin Cancer Res.* 2000;6:3095–3102.
39. Meredith RF, Khazaeli MB, Plott WE, et al. Phase II study of dual ^{131}I-labeled monoclonal antibody therapy with interferon in patients with metastatic colorectal cancer. *Clin Cancer Res.* 1996;2:1811–1818.
40. Wong JYC, Chu DZ, Yamauchi DM, et al. A phase I radioimmunotherapy trial evaluating ^{90}yttrium-labeled anti-carcinoembryonic antigen (CEA) chimeric T84.66 in patients with metastatic CEA-producing malignancies. *Clin Cancer Res.* 2000;6:3855–3863.
41. Alvarez RD, Huh WK, Khazaeli MB, et al. A phase I study of combined modality ^{90}yttrium-CC49 intraperitoneal radioimmunotherapy for ovarian cancer. *Clin Cancer Res.* 2002;8:2806–2811.
42. Wong JY, Shibata S, Williams LE, et al. A phase I trial of ^{90}Y-anti-carcinoembryonic antigen chimeric T84.66 radioimmunotherapy with 5-fluorouracil in patients with metastatic colorectal cancer. *Clin Cancer Res.* 2003;9:5842–5852.
43. Press OW, Eary JF, Appelbaum FR, et al. Radiolabeled-antibody therapy of B-cell lymphoma with autologous bone marrow support. *N Engl J Med.* 1993; 329:1219–1224.
44. Axworthy DB, Reno JM, Hylarides MD, et al. Cure of human carcinoma xenografts by a single dose of pretargeted yttrium-90 with negligible toxicity. *Proc Natl Acad Sci USA.* 2000;97:1802–1807.
45. Gautherot E, Rouvier E, Daniel L, et al. Pretargeted radioimmunotherapy of human colorectal xenografts with bispecific antibody and ^{131}I-labeled bivalent hapten. *J Nucl Med.* 2000;41:480–487.
46. Press OW, Corcoran M, Subbiah K, et al. A comparative evaluation of conventional and pretargeted radioimmunotherapy of CD20-expressing lymphoma xenografts. *Blood.* 2001;98:2535–2543.
47. Sharkey RM, McBride WJ, Karacay H, et al. A universal pretargeting system for cancer detection and therapy using bispecific antibody. *Cancer Res.* 2003;63: 354–363.
48. Fersht N, Vini L, A'Hern R, Harmer C. The role of radiotherapy in the management of elevated calcitonin after surgery for medullary thyroid cancer. *Thyroid.* 2001;11:1161–1168.